



Influence of the process on surface roughness of 3D-printed aluminum alloy AlSi40 parts

Dörfert, R.¹; Stoll, C.²; Freiße, H.¹; Seefeld, T.¹; Vollertsen, F.^{1,2}

¹BIAS - Bremer Institut für angewandte Strahltechnik GmbH, Klagenfurter Str. 5,
28359 Bremen, Germany

²University of Bremen, Bibliothekstr. 1, 28359 Bremen, Germany

Abstract: Selective Laser Melting (SLM) is a method of additive manufacturing enabling the production of complex parts directly from metal powder. Components manufactured by SLM typically have similar mechanical properties compared to conventionally manufactured ones. However, up to now surface roughness does not fulfill the criteria for a wide span of applications. Process strategies can be applied to influence the arithmetical mean height and the maximum height (S_a and S_z) of the surface roughness. By processing an AlSi40 alloy the impact of the main process parameters on resulting surface roughness, such as laser power, scan speed and focus position are investigated. The findings obtained of the experiments show a clear dependency of line energy and surface roughness in order to have a smooth surface roughness at a low line energy level of 0.8 J/mm compared to the necessary line energy of 6.7 J/mm to manufacture parts with high density. For the fabrication of AlSi40 parts with a density above 99.5% and a low surface roughness at the same time, it is feasible to separate the hatching and boundary parameters due to the difference between the required energy inputs.

Keywords: Aluminum alloy, AlSi40, high density, Selective Laser Melting, surface roughness

I. INTRODUCTION

Selective Laser Melting (SLM) enables the production of light weight structured components without the need for part specific tooling. It allows the production of parts with very complex geometries as well as the integration of additional functions like conformal cooling channels, which represent great challenges for conventional manufacturing methods. [1] SLM is a complex thermo-physical process that depends on materials, laser, scan, and environmental parameters [2]. It has been widely applied with different kinds of metal powders, such as stainless steel, titanium or aluminum alloys [3] and results in parts that have mechanical properties comparable to those of bulk materials [4]. In a layer-by-layer process SLM creates bulk parts by selectively melting and consolidating thin powder layers using a scan laser beam.

Aluminum (Al) alloys are some of the most common metal materials and are well suited for several lightweight applications e.g. automotive components for the reduction of fuel consumption [5]. In the field of additive manufacturing the most widespread alloys are of the 4xxx type containing silicon such as AlSi10Mg or AlSi12 and are complemented by scandium modified alloys (Scalmalloy®) [6], leading to parts with a density above 99.5% [7]. Further potential for light weight applications can enhance the necessary requirements on the used material. For instance the fabrication of aluminum cylinder bores does require an especially high wear resistance [8]. In addition, the current state of surface roughness for SLM generated parts requires excessive post processing methods to ensure quality expectations. Besides functional and aesthetic reasons the surface roughness has an impact on the fatigue strength [9]. Thus, light weight driven branches have to ensure the product quality with very cost and time consuming processes. The overall surface quality is highly depending on the chosen process parameters and part orientation and can either be dominated by partially melted powder particles or by the remelting process of previous melt tracks [10]. Up to now, the effects of the SLM process and powder parameters on the physical, mechanical and micro-structural properties of aluminum powders and its alloys are yet to be fully proven. There is little information available in literature about how to improve the surface quality of aluminum alloys. Low surface quality is one of the major shortcomings which prevent SLM to be adopted in wide applications although the SLM process provides many advantages compared to conventional machining [11].

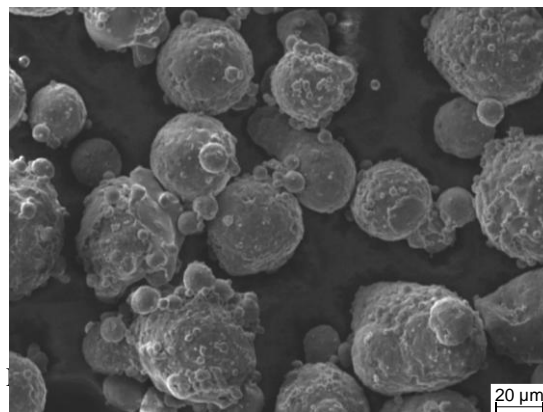
This paper addresses the improvement of surface quality and the determination of main influencing process parameters on surface roughness and density of an AlSi40 aluminum alloy processed via SLM.



II. EXPERIMENTAL

2.1 MATERIAL AND SLM PROCESS

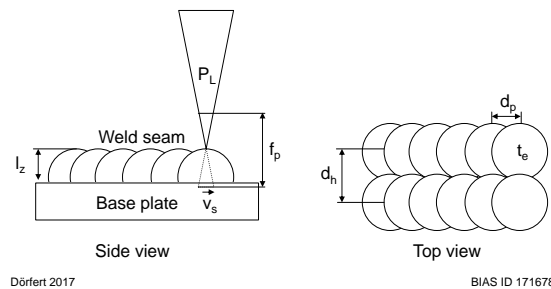
An AlSi40 aluminum alloy comprising 60 weight percent Al and 40 weight percent Si was investigated. AlSi40 is a hypereutectic alloy that contains silicon particles in a eutectic matrix. Pure silicon particles have high hardness and wear resistance as well as a lower thermal expansion compared to aluminum leading to a higher temperature range and a two phase solidification along with the high brittleness of local silicon concentrations resulting in a higher possibility for cracked parts and a higher surface roughness compared to near eutectic alloys such as AlSi10Mg. [8] Prior to the production of SLM parts, the powder was sieved with a 36 μm sieve to ensure a good flowability. The powder particles have a median particle size between 36 μm and 75 μm . Figure 1 shows the spherical morphology of the provided particles. A SLM - Realizer 250 machine with a 200 W IPG single mode fiber laser was used to produce the parts. The machine employs a fiber laser with a wavelength of 1073 nm. The standard beam diameter is 50 μm . Argon gas is used for the process atmosphere with a remaining oxygen content of 0.2%.



Dörfert 2017

BIAS ID 171070

The objective of the experiments was to optimize the process parameters to achieve the highest possible density as well as a low surface roughness. Therefore, the influence of the process parameters laser power P_L , scan speed v_s , hatch distance d_h that describes the spacing of the scan lines and focus position f_p on surface roughness and density were investigated (Figure 2). Scan speed can be further divided into two parts, named point distance d_p and the exposure time t_e . All experiments were conducted with a constant layer thickness l_z of 50 μm .



Dörfert 2017

BIAS ID 171678

Fig. 2 SLM process parameters

The focus position affects the laser spot size which changes the irradiance of parts' surface. It produces an effect on molten depth and forming. For a focus position of 0 μm the focus lies on surface of the current layer, whereas a negative value shifts the focus inside the layer and a value above 0 μm shifts the focus above the current layer respectively. The general processability of the AlSi40 powder was investigated within the parameter variations given in Table 1. For the measurement of the relative density cube shaped specimens with 10 mm edge length were fabricated. Via metallurgical cross sections the relative density was determined with a ZEISS AX10 microscope and the Image Access Enterprise V8 Software for particle analysis. The intended threshold d_{thr} for the relative density is above 99.5% and comparable to the achieved density of AlSi10Mg [7].



Table 1 AlSi40 Parameter Study

Parameter	Symbol	Setting
Laser power	P_L	120 W to 200 W
Scan speed	v_s	30 mm/s to 420 mm/s
Hatch distance	d_h	50 μm to 300 μm
Layer thickness	l_z	50 μm
Point distance	d_p	25 μm to 150 μm
Focus position	f_p	-100 μm to 100 μm

2.2 ROUGHNESS MEASUREMENT

Octagonal contour parts with a height of 10 mm were made for studying the surface roughness. By only building the contour of the octagonal parts, experimental time was reduced. The surface roughness was obtained on the lateral surfaces of the octagonal parts by means of 3D Laser Scanning Microscope VK-9700 from Keyence. Three pictures were taken from every side with a 10x magnification. The used confocal method is a contactless measurement and creates surface area topography information of the highly irregular surface of SLM generated parts [12]. The evaluation of the surface quality was expressed by the arithmetical mean height S_a and the maximum height S_z of the scale-limited surface [13].

III. RESULTS

3.1 RELATIVE DENSITY

The density of the parts machined with different laser power and scan speed values is exemplified by means of cross sections as shown in Figure 3. The relations among relative density, laser power and scan speed are shown in Figure 4a with a hatch distance of 150 μm . Parts fabricated with the highest possible laser power and low scan speed resulted in a relative density above 99.5%. Towards low laser power and high scan speed, the amount of porosity increases. For a constant laser power the highest density is achieved for low scan speed values.

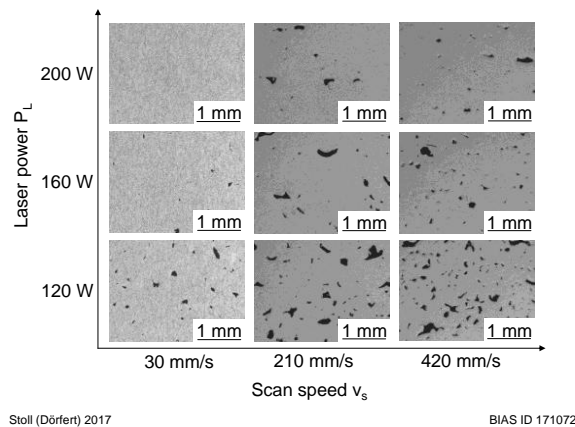
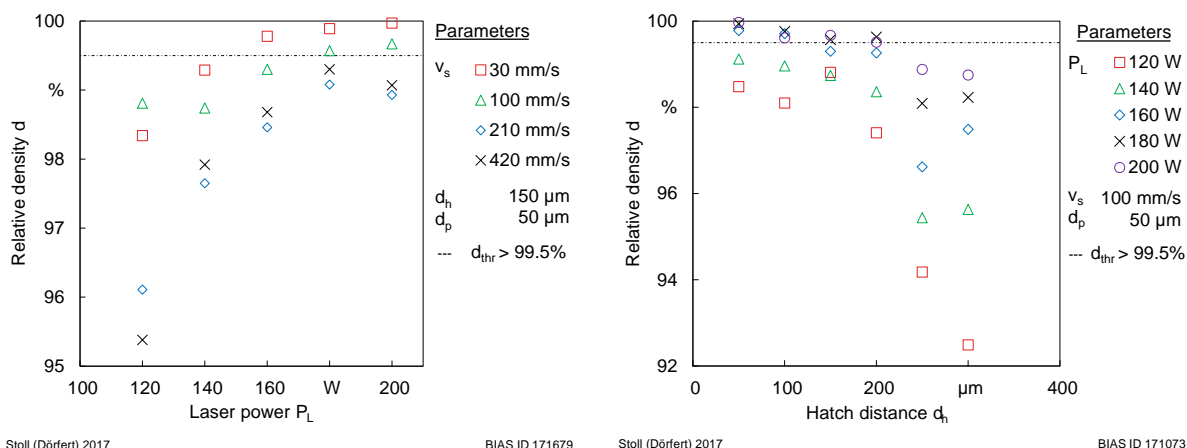


Fig. 3 Micrograph of SLM samples with scan speed and laser power

The influence of the hatch distance on the relative density is depicted in Figure 4b. When scan speed is constant, the relative density decreases with increasing hatch distance. This is caused by the increased gap between two successive tracks leading to insufficient connection. Furthermore, the relative density is reduced with decreasing laser power and fixed scan speed and hatch distance.



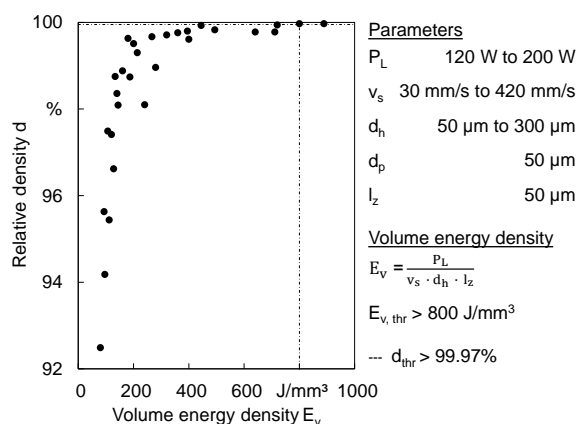
a) b)
 Fig. 4 Relative density as function of laser power and a) scan speed and b) hatch distance

Laser power and scan speed determine the energy supplied by the laser beam to solidify the powder material. The energy input per volume unit is defined as volume energy density E_v according to [14] and can be expressed as:

$$E_v = \frac{P_L}{v_s \cdot d_h \cdot l_z} \quad (1)$$

P_L	Laser power	W
v_s	Scan speed	mm/s
l_z	Layer thickness	μm
d_h	Hatch distance	μm

E_v is an experimental quantity that has large influence on part density. E_v decrease as the scan speed increases. Thus, if E_v is too low to melt the powder sufficiently, it will lead to porosity and low relative density [15]. The intended relative density of 99.5% was achieved by a large span of energy density values with a maximum value of 99.97%. Figure 5 displays the progression of increasing relative densities of the fabricated parts with increasing energy input. The necessary threshold $E_{v,thr}$ for a maximum relative density of 99.97% is 800 J/mm^3 and above.



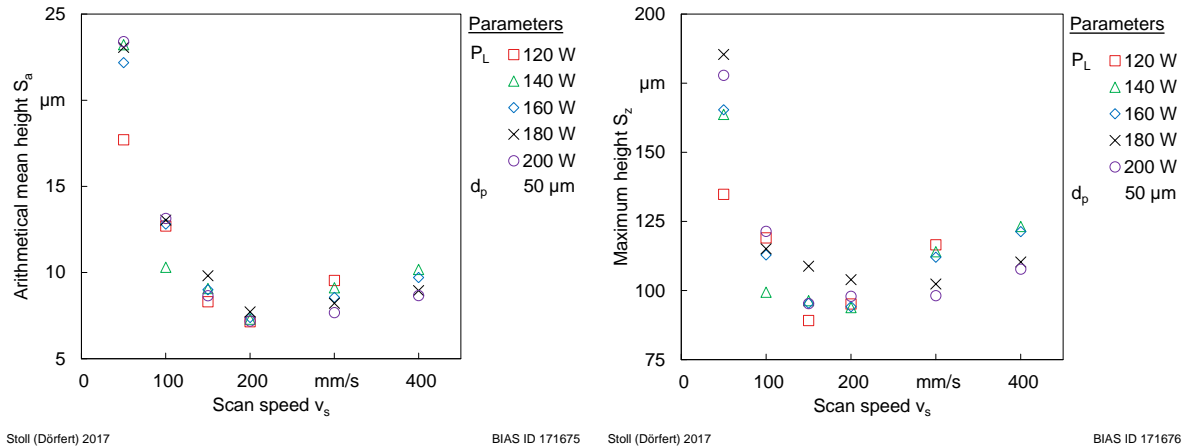
Stoll (Dörfert) 2017 BIAS ID 171677
 Fig. 5 Relation between volume energy density and relative density

3.2 SURFACE ROUGHNESS

The influence of the main process parameters laser power and scan speed on the surface roughness is displayed in Figure 6 for the arithmetical mean height S_a (6a) and for the maximum height S_z of the surface (6b).

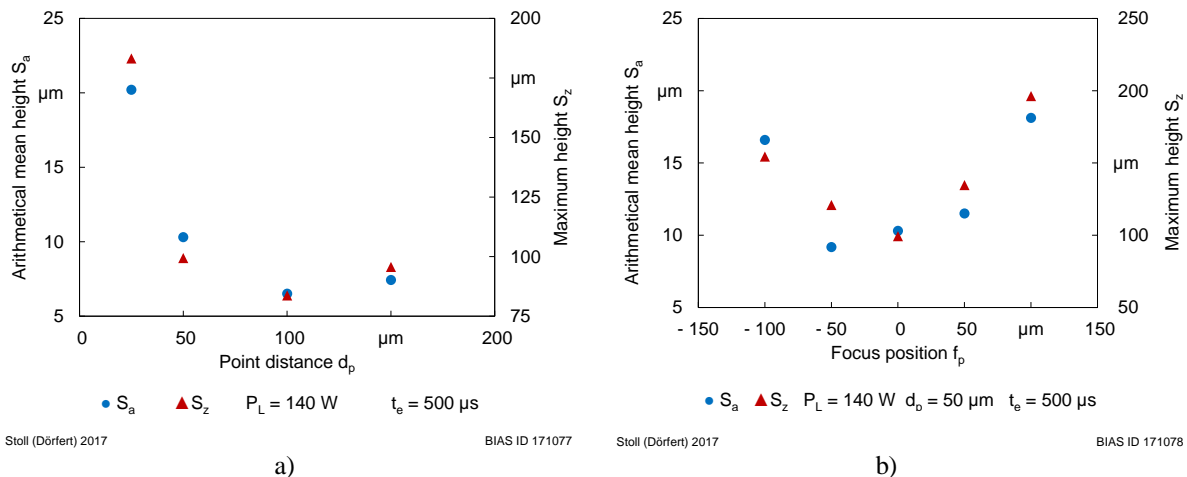


With increasing scan speed values the surface roughness is significantly reduced between 150 mm/s and 200 mm/s alongside an approximation of the roughness values for different laser powers. Thus, with increasing scan speed the influence of the laser power is less significant. Increasing v_s beyond 200 mm/s results in a steady increase of surface roughness. For very low scan speed values a low laser power leads to a lower surface roughness.



a) b)
 Fig. 6 Influence of laser power and scan speed on a) S_a and b) S_z

Besides the hatch distance for the overlapping of successive tracks the point distance influences the continuity of a single track due to the gap between the exposures of the laser beam spot on the powder and the resulting energy input. For a constant exposure time of 500 μs and a laser power of 140 W there is an inflection point at a point distance of 100 μm that provides the lowest surface roughness for a continuous track as shown in Figure 7a. The relation of focus position and surface roughness is shown in Figure 7b. There is no significant influence of the focus position from -50 μm to 50 μm , whereas for higher offset values of -100 μm and 100 μm the roughness increases.



a) b)
 Fig. 7 Relations of a) point distance and b) focus position on surface roughness

Furthermore, the main process parameters laser power and scan speed are related to the line energy E_L according to Equation (2). Exposure time t_e and point distance d_p are introduced to depict the scan speed with the following relation of Equation (3).

$$E_L = \frac{P_L}{v_s} \quad (2)$$

$$t_e = \frac{d_p}{v_s} \quad (3)$$



P_L	Laser power	W
v_s	Scan speed	mm/s
t_e	Exposure time	μ s
d_p	Point distance	μ m

Figure 8 shows the relation of line energy and surface roughness. Increasing line energy E_L up to 0.8 J/mm results in a decrease in S_a and S_z . However, the values of S_a and S_z increase while E_L varies from 0.8 J/mm to 4.5 J/mm. A minimum of S_a and S_z can be obtained of 6.65 μ m and 91.16 μ m. Overall, S_a and S_z will follow the same trend when varying process parameters.

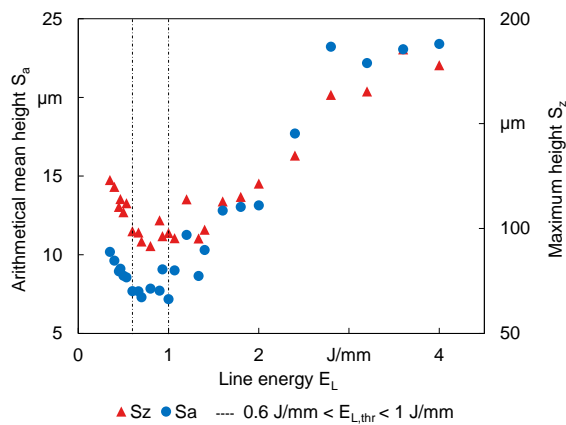


Fig. 8 Relation between line energy and surface roughness

IV. DISCUSSION

The fabrication of AlSi40-parts via SLM shows that several process parameters have to be adjusted accurately within a narrow window to achieve optimal combinations of material density and surface quality. Aluminum and aluminum alloys in general require a high energy input due to the high thermal conductivity and reflectivity [7]. Thus, low scan speed and high laser power result in parts with a relative density above 99.9% by applying a volume energy density E_v of 800 J/mm³ or a line energy of 6.7 J/mm respectively. However, the necessary energy input for the complete melting of the powder material based on the melting enthalpy and the bulk density is estimated with 1300 J/mm³. Thus, the experimental value of 800 J/mm³ within the given system parameters leads to high density parts but is not sufficient for a complete solidification of the powder particles.

Besides the relative density the energy input also has a significant impact on the parts' surface quality. Whereas a low energy density results in partially molten powder particles that are present on the parts' surface, very low scan speeds and high energy inputs leading to a large melt pool and consequently to a balling effect that reduces the surface quality [16]. Due to the incomplete solidification of the powder material partially molten powder particles on the parts' surface are likely the reason for the present surface roughness instead of balling phenomena. The surface finish is done during the solidification of the part's contour after the hatching of the volume for every layer. In order to reduce the surface roughness the partially molten powder particles present on the side walls have to be avoided or remelted during the boundary step without influencing the surrounding powder bed. Thus, if the solidification of the contour is done with a low line energy of 0.8 J/mm the heat conduction into the powder bed can be neglected leading to significantly lower surface roughness values due to surface-tension effects as usually applied by laser polishing [17]. Overall, it is a feasible approach to separate the hatching and boundary parameter sets with a line energy of 6.7 J/mm and 0.8 J/mm respectively in order to create high density AlSi40 parts with the lowest possible surface roughness.

V. CONCLUSION

The presented research demonstrates that with the aluminum alloy AlSi40 high density parts with an optimized surface quality can be fabricated. The high surface roughness is based on partially molten powder particles on the parts' side wall and can be greatly influenced during the boundary solidification with every layer. The parameter set for the boundary fabrication has to be precisely adjusted at a low level of line energy in



order to avoid the creation of new adherent powder particles during the polishing step due to unnecessary heat conduction into the powder bed.

VI. ACKNOWLEDGEMENTS

The authors are grateful for the financial support by the Senatorin für Wissenschaft, Gesundheit und Verbraucherschutz of the state of Bremen.

REFERENCES

- [1]. Hölker, R.; Jäger, A.; Ben Khalifa, N. & Tekkaya, A. E., *Controlling heat balance in hot aluminum extrusion by additive manufactured extrusion dies with conformal cooling channels*, International Journal of Precision Engineering and Manufacturing, 2013, 14, 1487-1493
- [2]. Neugebauer, F.; Keller, N.; Ploshikhin, V.; Feuerhahn, F. & Köhler, H., *Multi Scale FEM Simulation for Distortion Calculation in Additive Manufacturing of Hardening Stainless Steel*, Thermal Forming and Welding Distortion (IWOTE'14), eds.: F. Vollertsen, H. Tetzl, BIAS Verlag Bremen, 2014, 13-23
- [3]. Schmidt, M.; Merklein, M.; Bourell, D.; Dimitrov, D.; Hausotte, T.; Wegener, K.; Overmeyer, L.; Vollertsen, F. & Levy, G. N. , *Laser based additive manufacturing in industry and academia*, CIRP Annals - Manufacturing Technology, 2017, 66, 561 - 583
- [4]. Kruth, J. P.; L. Froyen, L.; Van Vaerenbergh, J.; Mercelis, P.; Rombouts, M. & Lauwers, B., *Selective laser melting of iron-based powder*, Journal of Materials Processing Technology, Volume 149, Issue 1, 2004, 616-622
- [5]. Zeiler, M.; Seefeld, T. & Vollertsen, F., *Influence of gap and edge offset on weld distortions by MIG-welding on aluminum alloys*, 3rd International Workshop on Thermal Forming and Welding Distortion (IWOTE'11), ed. F. Vollertsen. BIAS Verlag Bremen, 2011, 15 - 23
- [6]. Spierings, A. B.; Dawson, K.; Voegtlin, M.; Palm, F. & Uggowitzer, P. J., *Microstructure and mechanical properties of as-processed scandium-modified aluminium using selective laser melting*, CIRP Annals - Manufacturing Technology, 2016, 65, 213 - 216
- [7]. Buchbinder, D.; Schleifenbaum, H.; Heidrich, S.; Meiners, W. & Bültmann, J., *High Power Selective Laser Melting (HP SLM) of Aluminum Parts*, Physics Procedia, 2011, 12, 271 - 278
- [8]. Seefeld, T., *Laser-Randschichtschmelzen mit erhöhter Prozessgeschwindigkeit am Beispiel von Aluminium-Zylinderlaufbahnen*, Strahltechnik Band 42, eds.: F. Vollertsen, R. Bergmann. BIAS Verlag Bremen, 2011
- [9]. Wycisk, E.; Emmelmann, C.; Siddique, S. & Walther, F., *High Cycle Fatigue (HCF) Performance of Ti-6Al-4V Alloy Processed by Selective Laser Melting*, Manufacturing Science and Technology (ICMST2013), Trans Tech Publications, 2013, 816, 134-139
- [10]. Fox, J. C.; Moylan, S. P. & Lane, B. M., *Effect of Process Parameters on the Surface Roughness of Overhanging Structures in Laser Powder Bed Fusion Additive Manufacturing*, Procedia CIRP, 2016, 45, 131 - 134
- [11]. Townsend, A.; Senin, N.; Blunt, L.; Leach, R. & Taylor, J., *Surface texture metrology for metal additive manufacturing: a review* Precision Engineering, 2016, 46, 34 - 47
- [12]. Thompson, A.; Senin, N.; Giusca, C. & Leach, R., *Topography of selectively laser melted surfaces: A comparison of different measurement methods*, CIRP Annals - Manufacturing Technology, 2017, 66, 543 - 546
- [13]. ISO 25178-2:2012 *Geometrical Product Specifications (GPS)—Surface Texture: Areal - Part 2: Terms, Definitions and Surface Texture Parameters*
- [14]. VDI-Richtlinie: *VDI 3405 Blatt 2 Additive Fertigungsverfahren - Strahlschmelzen metallischer Bauteile - Qualifizierung, Qualitätssicherung und Nachbearbeitung*
- [15]. Simchi, A., *Direct laser sintering of metal powders: Mechanism, kinetics and microstructural features*, Materials Science and Engineering: A, 2006, 428, 148 - 158
- [16]. Louvis, E.; Fox, P. & Sutcliffe, C. J., *Selective laser melting of aluminium components*, Journal of Materials Processing Technology, 2011, 211, 275 - 284
- [17]. Pfefferkorn, F. E. & Morrow, J.D., *Controlling surface topography using pulsed laser micro structuring*, CIRP Annals - Manufacturing Technology, 2017, 66, 241 - 244